Nonlinear Dyn (2008) 54: 395–408
DOI 10.1007/s11071-008-9338-2

ORIGINAL PAPER

Exact solution and stability of postbuckling configurations of beams

Ali H. Nayfeh · Samir A. Emam

Received: 17 March 2006 / Accepted: 2 January 2008 / Published online: 23 February 2008

Abstract We present an exact solution for the postbuckling configurations of beams with fixed–fixed, fixed–hinged, and hinged–hinged boundary conditions. We take into account the geometric nonlinearity arising from midplane stretching, and as a result, the governing equation exhibits a cubic nonlinearity. We solve the nonlinear buckling problem and obtain a closed-form solution for the postbuckling configurations in terms of the applied axial load. The critical buckling loads and their associated mode shapes, which are the only outcome of solving the linear buckling problem, are obtained as a byproduct. We investigate the dynamic stability of the obtained postbuckling configurations and find out that the first buckled shape is a stable equilibrium position for all boundary conditions. However, we find out that buckled configurations beyond the first buckling mode are unstable equilibrium positions. We present the natural frequencies of the lowest vibration modes around each of the first three buckled configurations. The results show that many internal resonances might be activated among the vibration modes around the same as well as different buckled configurations. We present preliminary results of the dynamic response of a fixed–fixed beam in the case of a one-to-one internal resonance between the first vibration mode around the first buckled configuration and the first vibration mode around the second buckled configuration.

Keywords Exact solution · Stability · Free vibration · Buckled beams

A.H. Nayfeh (✉)
Department of Engineering Science and Mechanics, MC 0219, Virginia Polytechnic Institute and State University, Blacksburg, VA 24061, USA
e-mail: anayfeh@vt.edu

S.A. Emam
Department of Mechanical Design and Production, Faculty of Engineering, Zagazig University, Zagazig 44519, Egypt

1 Background

Buckling is a static instability of structures due to in-plane loading. Buckling was first introduced by Euler more than two centuries ago. Since then, the main concern of the investigations of buckling problems was to find the critical buckling loads and their associated mode shapes. When the geometric nonlinearity, which accounts for midplane stretching, is taken into consideration, one obtains the nonlinear buckling problem. Solving the nonlinear buckling problem for a given axial load results in the postbuckling configurations. Numerical solutions for the nonlinear buckling problem are available in the literature. In this study, an exact solution for the postbuckling problem is presented. The critical buckling loads and their associated mode shapes are obtained as a byproduct.

There is a large number of papers dealing with the analysis of buckling problems, however, to the best of

the authors' knowledge, there is no exact solution for the postbuckling of beams loaded by axial loads beyond the critical buckling loads. Numerical solutions for the postbuckling problem are available in the literature. For a detailed review of the vibrations of buckled beams, we refer the reader to Emam [1] and Nayfeh and Pai [2]. The objectives of the present paper are four folds. The first is to obtain a closed-form solution for the postbuckling configurations as a function of the applied axial load. The second is to investigate the stability of the higher postbuckling configurations. The third is to determine the natural frequencies of vibrations around the buckled configurations. The fourth is to present preliminary results for the nonlinear interaction between modes of vibration around different buckled configurations. Next, we discuss two of the publications related to the objectives of this paper.

Fang and Wickert [3] investigated the static deformation of micromachined beams in the prebuckling, transition, and postbuckling states under prescribed inplane compressive stresses using analytical and experimental means. They developed the governing equation of a geometrically nonlinear imperfect beam. They assumed a shape for the postbuckled configuration in the form of the first buckling mode and obtained the amplitude of the postbuckling configuration. Li and Zhou [4] investigated free vibrations of a thermally buckled beam taking into account the geometric nonlinearity in the prebuckling and postbuckling ranges. They used a shooting method to solve for the postbuckling configurations and the linear vibration modes of prebuckled and postbuckled beams.

In this paper, we present the governing equation and boundary conditions of fixed–fixed, fixed–hinged, and hinged–hinged laterally deflected beams taking into account the geometrical nonlinearity. We solve the nonlinear postbuckling problem and obtain a closed-form solution for the buckled configurations as a function of the applied axial load. To show the onset of buckling, we plot the static deflection against the applied axial load.

We follow Nayfeh et al. [5] and obtain an exact solution for the free vibration problem around the buckled configurations. We calculate the lowest frequencies of vibration around each of the buckled configurations. We find out that the first buckled configuration is a stable equilibrium position for all boundary conditions. However, buckled shapes beyond the first buckling shape are found to be unstable. We plot the lowest natural frequencies for the prebuckled and postbuckled configurations. The fundamental natural frequency in the prebuckled configuration decreases as the applied axial load is increased. At the onset of buckling, the fundamental frequency vanishes. However, as the beam buckles, its fundamental natural frequency increases as the applied load is increased. Moreover, we find many possible internal resonances among vibration modes around the same buckled configuration as well as vibration modes around different buckled configurations. We note that for axial loads beyond the second critical load, the dynamics of the postbuckled beam are rich and complex. We present preliminary results of the nonlinear coupling via a one-to-one internal resonance between the first vibration mode around the first buckled configuration and the first vibration mode around the second buckled configuration. This investigation opens the door for more theoretical and experimental investigations of the dynamics of buckled beams.

2 Problem formulation

The problem governing the transverse vibration of beams accounting for midplane stretching is given by [1, 2]

$$m\frac{\partial^2\hat{w}}{\partial\hat{t}^2}+\hat{P}\frac{\partial^2\hat{w}}{\partial\hat{x}^2}+EI\frac{\partial^4\hat{w}}{\partial\hat{x}^4}+\hat{\mu}\frac{\partial\hat{w}}{\partial\hat{t}} =\frac{EA}{2\ell}\frac{\partial^2\hat{w}}{\partial\hat{x}^2}\int_0^{\ell}\left(\frac{\partial\hat{w}}{\partial\hat{x}}\right)^2 d\hat{x}+\hat{F}(\hat{x})\cos\hat{\Omega}\hat{t} \tag{1}$$

subject to the boundary conditions

$$\hat{w}=0 \quad \text{and} \quad \frac{\partial\hat{w}}{\partial\hat{x}}=0 \quad \text{at } \hat{x}=0,\ell \tag{2}$$

for fixed–fixed beams,

$$\hat{w}=0 \quad \text{and} \quad \frac{\partial^2\hat{w}}{\partial\hat{x}^2}=0 \quad \text{at } \hat{x}=0,\ell \tag{3}$$

for hinged–hinged beams, and

$$\hat{w}=0 \quad \text{and} \quad \frac{\partial\hat{w}}{\partial\hat{x}}=0 \quad \text{at } \hat{x}=0, \tag{4a}$$

$$\hat{w}=0 \quad \text{and} \quad \frac{\partial^2\hat{w}}{\partial\hat{x}^2}=0 \quad \text{at } \hat{x}=\ell \tag{4b}$$

for fixed–hinged beams. Here, m is the mass per unit undeformed length; $\hat{w}(\hat{x},\hat{t})$ is the transverse displacement at position $\hat{x}$ and time $\hat{t}$; E is Young's modulus;

A and I are the area and moment of inertia of the cross section, respectively; ℓ is the undeformed length of the beam; $\hat{P}$ is the axial load; $\hat{\mu}$ is the damping coefficient; $\hat{F}$ is the spatial distribution of the transverse load; and $\hat{\Omega}$ is its frequency. For convenience, we use the following nondimensional variables:

$$x = \frac{\hat{x}}{\ell}, \qquad w = \frac{\hat{w}}{r}, \qquad t = \hat{t}\sqrt{\frac{EI}{m\ell^4}},$$

$$\Omega = \hat{\Omega}\sqrt{\frac{m\ell^4}{EI}}$$

where $r = \sqrt{I/A}$ is the radius of gyration of the cross section. As a result, we rewrite (1)–(4) as

$$\ddot{w} + w^{iv} + Pw'' + \mu\dot{w} - \frac{1}{2}w''\int_0^1 w'^2\,dx = F(x)\cos\Omega t. \tag{5}$$

$$w = 0 \quad \text{and} \quad w' = 0 \quad \text{at } x = 0, 1, \tag{6}$$

$$w = 0 \quad \text{and} \quad w'' = 0 \quad \text{at } x = 0, 1, \tag{7}$$

$$w = 0 \quad \text{and} \quad w' = 0 \quad \text{at } x = 0, \tag{8a}$$

$$w = 0 \quad \text{and} \quad w'' = 0 \quad \text{at } x = 1 \tag{8b}$$

where the overdot indicates the derivative with respect to t, the prime indicates the derivative with respect to x, and

$$P = \frac{\hat{P}\ell^2}{EI}, \qquad \mu = \frac{\hat{\mu}\ell^2}{\sqrt{mEI}}, \qquad F = \frac{\hat{F}\ell^4}{rEI}$$

are nondimensional quantities.

3 Buckling problem

In the case of fixed–fixed beams, the buckling problem can be obtained from (5) and (6) by dropping the time-dependent, damping, and forcing terms and denoting the buckled configuration by $\psi(x)$. The result is

$$\psi^{iv} + P\psi'' - \frac{1}{2}\psi''\int_0^1 \psi'^2\,dx = 0, \tag{9}$$

$$\psi = 0 \quad \text{and} \quad \psi' = 0 \quad \text{at } x = 0, 1. \tag{10}$$

We note that the integral in (9) is a constant for a given $\psi(x)$. Hence, we let

$$\Gamma = \frac{1}{2}\int_0^1 \psi'^2\,dx \tag{11}$$

where Γ is a constant. As a result, (9) reduces to

$$\psi^{iv} + \lambda^2\psi'' = 0 \tag{12}$$

where $\lambda^2 = P - \Gamma$ is a constant that represents a critical buckling load. Equation (12) is a fourth-order ordinary-differential equation with constant coefficients whose general solution is given by

$$\psi(x) = c_1 + c_2 x + c_3\cos\lambda x + c_4\sin\lambda x \tag{13}$$

where the c_i are constants. Satisfying the boundary conditions by substituting (13) into (10) yields the following four algebraic equations:

$$c_1 + c_3 = 0, \tag{14}$$

$$c_2 + \lambda c_4 = 0, \tag{15}$$

$$c_1 + c_2 + c_3\cos\lambda + c_4\sin\lambda = 0, \tag{16}$$

$$c_2 - \lambda c_3\sin\lambda + c_4\lambda\cos\lambda = 0. \tag{17}$$

Equations (14)–(17) represent an eigenvalue problem for λ. Demanding that the determinant of the coefficient matrix equals zero, we obtain the following characteristic equation for λ:

$$2 - 2\cos\lambda - \lambda\sin\lambda = 0. \tag{18}$$

Solving (18) for λ yields 2π, 8.9868, 4π, and 15.4505 as the first four eigenvalues. Then, it follows from (14)–(17) that the corresponding mode shapes $\psi(x)$ are given by

$$\psi(x) = c\left[1 - \frac{\lambda(1-\cos\lambda)}{\lambda - \sin\lambda}x - \cos\lambda x + \frac{1-\cos\lambda}{\lambda - \sin\lambda}\sin\lambda x\right] \tag{19}$$

where c is a constant to be determined. The expression $\psi(x)$ governs both symmetric and antisymmetric buckling shapes. Next, we give separate expressions for symmetric and antisymmetric modes.

We manipulate (18) using trigonometric identities as follows:

$$2-2\cos\lambda-\lambda\sin\lambda$$
$$=4\sin^2\frac{\lambda}{2}-2\lambda\sin\frac{\lambda}{2}\cos\frac{\lambda}{2}$$
$$=4\sin\frac{\lambda}{2}\left(\sin\frac{\lambda}{2}-\frac{\lambda}{2}\cos\frac{\lambda}{2}\right)=0. \tag{20}$$

It follows from (20) that there are two cases. First,

$$\sin\frac{\lambda}{2}=0 \quad \text{or} \quad \lambda=2m\pi \quad \text{where } m=1,2,\ldots \tag{21}$$

and (19) yields the symmetric mode shapes

$$\psi(x)=c\big[1-\cos(2m\pi x)\big]. \tag{22}$$

Second,

$$\tan\frac{\lambda}{2}=\frac{\lambda}{2} \tag{23}$$

and (19) yields the antisymmetric mode shapes

$$\psi(x)=c\left[1-2x-\cos\lambda x+\frac{2}{\lambda}\sin\lambda x\right] \tag{24}$$

because

$$\frac{1-\cos\lambda}{\lambda-\sin\lambda}=\frac{2\sin^2\frac{\lambda}{2}}{2\tan\frac{\lambda}{2}-2\sin\frac{\lambda}{2}\cos\frac{\lambda}{2}}=\frac{\sin\frac{\lambda}{2}\cos\frac{\lambda}{2}}{1-\cos^2\frac{\lambda}{2}}$$
$$=\cot\frac{\lambda}{2}=\frac{2}{\lambda}.$$

To this point, the buckled configuration $\psi(x)$ satisfies the boundary conditions, but there is a condition that has not been satisfied yet; that is, the relation

$$\lambda^2=P-\Gamma=P-\frac{1}{2}\int_0^1\psi'^2\,dx. \tag{25}$$

Substituting (19) into (25), making use of (18), and using trigonometric identities, we obtain

$$\lambda^2=P-\frac{1}{4}c^2\lambda^2 \quad \text{or} \quad c=\pm2\sqrt{\frac{P}{\lambda^2}-1}. \tag{26}$$

Thus, for a given axial load P, the constant c corresponding to any eigenvalue λ can be determined, and hence its corresponding buckled shape can be obtained. To show a numerical example, let $P=10\pi^2$ that is beyond the second critical buckling load, the constant c corresponding to the first and second buckled shapes is given by ±2.4495 and ±0.4924, respectively. The corresponding buckled shapes can then be expressed as

$$\psi_1(x)=\pm2.4495(1-\cos2\pi x),$$
$$\psi_2(x)=\pm0.9424\left(1-2x-\cos\lambda_2 x+\frac{2}{\lambda_2}\sin\lambda_2 x\right)$$

where $\lambda_2=8.9868$.

We show in Appendix A that the buckled mode shapes satisfy the orthogonality condition

$$\int_0^1\psi_1'\psi_2'\,dx=0 \tag{27}$$

where ψ_1 and ψ_2 are two mode shapes corresponding to the different eigenvalues λ_1 and λ_2, respectively. This orthogonality condition holds for all boundary conditions treated in this paper.

In the case of fixed–hinged beams, (10) is replaced with

$$\psi=0 \quad \text{and} \quad \psi'=0 \quad \text{at } x=0, \tag{28}$$

$$\psi=0 \quad \text{and} \quad \psi''=0 \quad \text{at } x=1. \tag{29}$$

It follows from (13), (28), and (29) that

$$\psi(x)=c\left[1-x-\cos\lambda x+\frac{\sin\lambda x}{\sin\lambda}\right] \tag{30}$$

where

$$\sin\lambda-\lambda\cos\lambda=0. \tag{31}$$

Again, substituting (30) into (25) and using (31) yields (26).

In the case of hinged–hinged beams, (10) is replaced with

$$\psi=0 \quad \text{and} \quad \psi''=0 \quad \text{at } x=0,1. \tag{32}$$

Then the characteristic equation becomes

$$\sin\lambda=0 \tag{33}$$

yielding the critical buckling loads $m^2\pi^2$, where m is an integer. Hence, the mode shapes are given by

$$\psi(x)=c\sin(m\pi x). \tag{34}$$

Substituting (34) into (25) yields the same postbuckling relation given by (26). Surprisingly, the constant c for all of the boundary conditions is related to the

Table 1 Critical buckling loads for various boundary conditions

Boundary conditions	Fixed–Fixed	Fixed–Hinged	Hinged–Hinged
Characteristic equation	$2-2\cos\lambda-\lambda\sin\lambda=0$	$\lambda\cos\lambda-\sin\lambda=0$	$\sin\lambda=0$
λ^2/π^2	4, 8.18, 16, 24.19	2.05, 6.05, 12.05, 20.05	1, 4, 9, 16

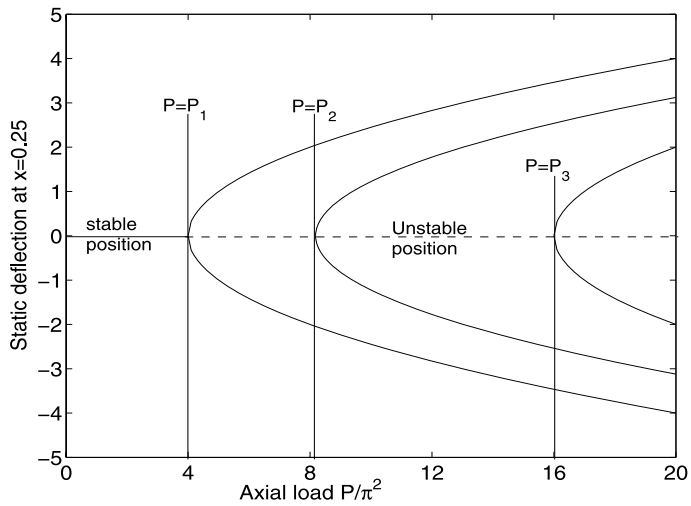

Fig. 1 Bifurcation diagram for the static deflection of a fixed–fixed beam at $x=0.25$ with the axial load showing the first three buckled configurations

applied axial load P by the same relation, (26). In Table 1, we list the lowest four critical buckling loads and the corresponding characteristic equations.

In Fig. 1, we show the static bifurcation diagram for the first three buckled configurations of a fixed–fixed beam, where we plot the deflection at one-fourth of the span against the axial load. As the axial load exceeds the first critical buckling load, $P_1=4\pi^2$, the straight position loses stability and the beam buckles. As the axial load is increased beyond the second critical buckling load, $P_2=8.18\pi^2$, the beam has three equilibria: the straight configuration, which is unstable, and two others corresponding to the first and second buckled configurations. The stability of the latter equilibria are determined in the next section. We emphasize that these buckled configurations are exact. As the axial load is increased beyond the third critical buckling load, $P_3=16\pi^2$, the beam exhibits three nontrivial equilibria corresponding to the three buckled configurations as shown in Fig. 1.

To relate the critical buckling load to the frequencies of vibrations around the undeflected position, we solve the linear vibration problem given by (5) and (6), where the damping, forcing, and nonlinear terms are neglected. Figure 2 shows variation of the lowest three natural frequencies with the axial load. We note that as the axial load reaches the first critical buckling value, the first natural frequency approaches zero, and hence the undeflected position becomes unstable. Beyond this critical buckling load, the straight configuration loses stability and the beam acquires another stable equilibrium positions, which are the buckled configurations. Similar trends are obtained for the higher buckling modes. This result is well known in the literature; however, we present it here to eliminate any confusion that might arise when we present the frequencies of vibration around the buckled configurations. In the latter case, the vibration frequencies increase as the axial load is increased, as shown in the next section.

4 Stability of buckled configurations

To investigate the dynamic stability of a buckled configuration, we introduce a small disturbance and determine the time evolution of that disturbance. To this end, we let

$$w(x,t)=\psi(x)+v(x,t) \tag{35}$$

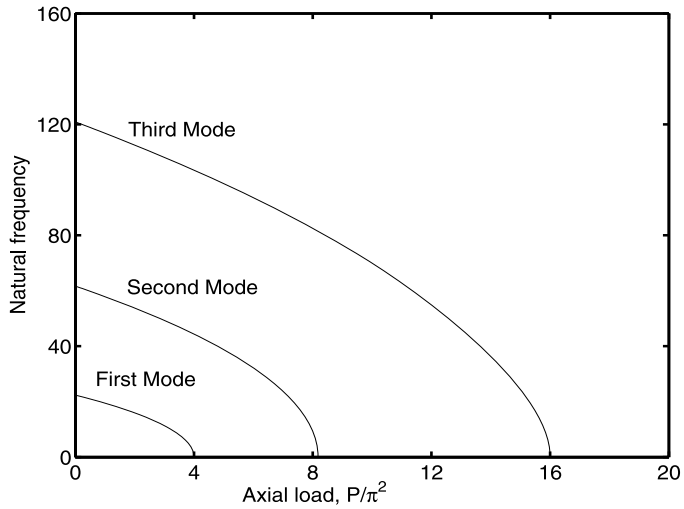

Fig. 2 Variation of the lowest three natural frequencies around the undeflected position with the axial load for a fixed–fixed beam

where $v(x,t)$ is a small dynamic disturbance around the buckled configuration $\psi(x)$. Substituting (35) into (5) and (6) and using (9) and (10), we obtain for fixed–fixed beams

$$\ddot{v} + v^{iv} + \lambda^2 v'' + \mu\dot{v} = \psi'' \int_0^1 \psi' v'\,dx + \frac{1}{2}\psi'' \int_0^1 v'^2\,dx + v'' \int_0^1 \psi' v'\,dx + \frac{1}{2}v'' \int_0^1 v'^2\,dx + F\cos\Omega t, \tag{36}$$

$$v = 0 \quad \text{and} \quad v' = 0 \quad \text{at } x = 0, 1. \tag{37}$$

The linear free vibration problem can be obtained by dropping the nonlinear, damping, and forcing terms from (36); the result is

$$\ddot{v} + v^{iv} + \lambda^2 v'' = \psi'' \int_0^1 \psi' v'\,dx. \tag{38}$$

We let

$$v(x,t) = \phi(x)e^{i\omega t} \tag{39}$$

where ω is a natural frequency and $\phi(x)$ is its corresponding mode shape. Substituting (39) into (38) and (37), we obtain

$$\phi^{iv} + \lambda^2\phi'' - \omega^2\phi = \psi'' \int_0^1 \psi'\phi'\,dx, \tag{40}$$

$$\phi = 0 \quad \text{and} \quad \phi' = 0 \quad \text{at } x = 0, 1. \tag{41}$$

Equation (40) is a nonhomogeneous fourth-order ordinary-differential equation with constant coefficients whose general solution can be expressed as

$$\phi(x) = \phi_h(x) + \phi_p(x) \tag{42}$$

where the homogeneous solution ϕ_h is governed by

$$\phi_h^{iv} + \lambda^2\phi_h'' - \omega^2\phi_h = 0 \tag{43}$$

and the particular solution ϕ_p is governed by

$$\phi_p^{iv} + \lambda^2\phi_p'' - \omega^2\phi_p = \psi'' \int_0^1 \psi'\phi_h'\,dx + \psi'' \int_0^1 \psi'\phi_p'\,dx. \tag{44}$$

The general solution of (43) can be expressed as

$$\phi_h(x) = d_1\sin s_1 x + d_2\cos s_1 x + d_3\sinh s_2 x + d_4\cosh s_2 x \tag{45}$$

where the d_i are constants and

$$s_{1,2} = \left[\pm\frac{1}{2}\lambda^2 + \frac{1}{2}\sqrt{\lambda^4 + 4\omega^2}\right]^{\frac{1}{2}}. \tag{46}$$

Because the second integral on the right-hand side of (44) is constant for given $\psi(x)$ and $\phi_p(x)$, a particular solution of (44) has the form

$$\phi_p(x) = d_5\psi''. \tag{47}$$

Substituting (47) into (44) yields

$$d_5\left(\psi^{vi}+\lambda^2\psi^{iv}\right)-d_5\omega^2\psi''$$
$$=\psi''\Lambda+d_5\psi''\int_0^1\psi'\psi'''\,dx \tag{48}$$

where

$$\Lambda=\int_0^1\psi'\phi_h'\,dx \tag{49}$$

is a constant.

We note that the term between the parenthesis on the left-hand side of (48) vanishes identically by virtue of (12). As a result, (48) reduces to

$$\Lambda+d_5\left(\omega^2+\int_0^1\psi'\psi'''\,dx\right)=0. \tag{50}$$

There are two possibilities: either $\Lambda=0$ or $\Lambda\neq 0$. In the first case, the derivative of the buckling mode shape is orthogonal to the derivative of the vibration mode shape, and hence (50) yields either

$$d_5=0 \tag{51}$$

or

$$\omega^2=-\int_0^1\psi'\psi'''\,dx=\int_0^1\psi\psi^{iv}\,dx$$
$$=-\lambda^2\int_0^1\psi\psi''\,dx=\lambda^2\int_0^1\psi'^2\,dx$$
$$=\frac{1}{2}\lambda^4c^2=2\lambda^4\left(\frac{P}{\lambda^2}-1\right). \tag{52}$$

When $d_5=0$, the vibration mode shapes are given by only the homogeneous solution. These are called the even modes; they do not depend on the applied axial load as shown below. When $\Lambda\neq 0$, (50) provides an extra equation for the constants d_i. We note this possibility holds for all boundary conditions since it is derived from the equation of motion.

The general solution of (40) can be expressed as follows:

$$\phi(x)=d_1\sin s_1x+d_2\cos s_1x$$
$$+d_3\sinh s_2x+d_4\cosh s_2x+d_5\psi''. \tag{53}$$

Applying the boundary conditions, given by (41), we obtain

$$d_2+d_4+d_5c\lambda^2=0, \tag{54}$$

$$s_1\,d_1+s_2\,d_3-d_5c\lambda^2\left[\frac{\lambda(1-\cos\lambda)}{\lambda-\sin\lambda}\right]=0, \tag{55}$$

$$d_1\sin s_1+d_2\cos s_1+d_3\sinh s_2$$
$$+d_4\cosh s_2+d_5c\lambda^2\left[\cos\lambda-\sin\lambda\frac{1-\cos\lambda}{\lambda-\sin\lambda}\right]=0, \tag{56}$$

$$d_1\,s_1\cos s_1-d_2\,s_1\,\sin s_1$$
$$+d_3\,s_2\,\cosh s_2+d_4\,s_2\sinh s_2$$
$$-d_5c\lambda^2\left[\lambda\sin\lambda+\lambda\frac{\cos\lambda-\cos^2\lambda}{\lambda-\sin\lambda}\right]=0. \tag{57}$$

Equations (54)–(57) and either (50) or (51) constitute a system of five homogeneous algebraic equations for the constants d_i. We emphasize that this system of equations applies for both symmetric and antisymmetric buckling configurations. Solving this eigenvalue problem, we obtain the natural frequencies ω and their corresponding vibration mode shapes ϕ around a buckled configuration $\psi(x)$ due to a given axial load P.

For a stable buckled configuration, ω^2 must be positive, and hence ω is real. Therefore, to examine the stability of the buckled configurations, we calculated variation of the vibration frequencies with the axial load for the three cases of fixed–fixed, fixed–hinged, and hinged–hinged boundary conditions.

For a fixed–fixed beam, we let $P=1.0025P_1$, which results in only the first bucked shape, and calculated the numerical values of ω^2 in two ranges: $-10{,}000\leq\omega^2\leq 0$ and $\omega^2>0$. Searching for roots in the first range yields only one root that is given by $\omega^2=-389.636$. Solving the eigenvalue problem for its corresponding mode shape, we find out that this negative root corresponds to a nonphysical shape; in other words, it corresponds to a vanishing mode shape. In the second range, the first three positive roots are given by 2.597, 1968.05, and 10,711, respectively. We find out that all of the positive roots correspond to physical mode shapes. As a result, we conclude that the first buckled configuration is a stable equilibrium position.

To investigate the stability of the second buckled shape, we let $P=1.0025P_2$, which ensures the existence of the second buckled shape. In the range $-10{,}000\leq\omega^2\leq 0$, we detect two negative roots: $\omega^2=-581.416$ and $\omega^2=-1630.66$. Investigating their corresponding mode shapes, we find out that

the second negative root corresponds to a vanishing mode shape and the first negative root corresponds to a physical buckled shape. Therefore, the second buckled shape is an unstable equilibrium position.

Repeating the same procedure for the third buckled shape, we obtain two negative roots: $\omega^2 = -3931.52$ and $\omega^2 = -6234.18$. The first root yields a physical mode shape and as a result, the third buckled shape is an unstable equilibrium position.

In Fig. 3(a), we show variation of the lowest four vibration frequencies around the first buckled configuration with the axial load. Solid lines indicate odd vibration modes and dotted lines indicate even ones. For vibrations around higher-buckling modes, we note that odd modes are not always symmetric and even modes are not always antisymmetric. This is because the first vibration mode around a buckling configuration is similar in shape to that buckled configuration; that is, the first vibration mode around the first buckled configuration is symmetric and the first vibration mode around the second buckled configuration is antisymmetric. This is expected since we deal with small vibrations, which are close to the buckled configuration they vibrate around.

Figures 3(b) and 3(c) show variation of the lowest vibration frequencies around the second and third buckled configurations with the axial load. Figures 3(a), 3(b), and 3(c) show that internal resonances, such as one-to-one, two-to-one, and three-to-one, might be activated between vibration modes around the same buckled configuration. To investigate the possibility of activating internal resonances between vibration modes around different buckled configurations, we plot all natural frequencies, as shown in Fig. 3(d). We note that nonlinear interactions are possible not only among vibration modes around the same buckled configuration, but also around different buckled configurations. This means that we are dealing with a nonlinear system having stable and unstable equilibrium positions that might be coupled via internal resonances. This indicates that the beam exhibits rich dynamics as the axial load exceeds the second buckling load.

In what follows, we use two indices to identify the natural frequencies and their corresponding mode shapes. For example, ω_{ij} denotes the natural frequency of the ith vibration mode around the jth buckled configuration. A quick inspection of Fig. 3 indicates that a one-to-one internal resonance might be activated between ϕ_{11} and ϕ_{12} at $P = 9.5\pi^2$.

For a fixed–hinged beam, we use the same procedure used for fixed–fixed beams. Demanding that the mode shapes $\phi(x)$ satisfy the fixed–hinged boundary conditions yields the following four equations:

$$d_2 + d_4 + c\,d_5\lambda^2 = 0, \tag{58}$$

$$d_1 \sin s_1 + d_2 \cos s_1 + d_3 \sinh s_2 + d_4 \cosh s_2 = 0, \tag{59}$$

$$d_1 s_1 + d_3 s_2 - c\,d_5\lambda^2 = 0, \tag{60}$$

$$d_1 s_1^2 \sin s_1 + d_2 s_1^2 \cos s_1 - d_3 s_2^2 \sinh s_2 - d_4 s_2^2 \cosh s_2 = 0. \tag{61}$$

These equations along with either (50) or (51) constitute an eigenvalue problem for the natural frequencies of vibration around the buckled configurations of fixed–hinged beams.

To investigate the stability of buckled configurations of fixed–hinged beams, we let $P = 1.0025P_1$, and investigate the stability of the first buckled shape. We find only one negative root that is given by $\omega^2 = -101.92$. However, this negative root corresponds to a vanishing mode shape. All positive roots correspond to physical mode shapes, and as a result the first buckled configuration is a stable equilibrium position. To investigate the stability of the second and third buckled configurations, we increase the axial load and compute the natural frequency ω^2. In each case, we find a negative root that corresponds to a physical mode shape, and hence the second and third buckled shapes are unstable equilibrium positions. Figure 4 presents variation of the natural frequencies of vibration around the first, second, and third buckled configurations. Many internal resonances might be activated among vibration modes around the same buckled configuration as well as around different buckled configurations. An interesting one-to-one internal resonance among three modes, namely ϕ_{21}, ϕ_{12}, and ϕ_{13}, of a fixed–hinged buckled beam might be activated at $P \approx 14.6\pi^2$, as shown in Fig. 4(d).

Similarly, the four equations satisfying the boundary conditions of hinged–hinged beams are given by

$$d_2 + d_4 = 0, \tag{62}$$

$$d_2 s_1^2 - d_4 s_2^2 = 0, \tag{63}$$

$$d_1 \sin s_1 + d_2 \cos s_1 + d_3 \sinh s_2 + d_4 \cosh s_2 = 0, \tag{64}$$

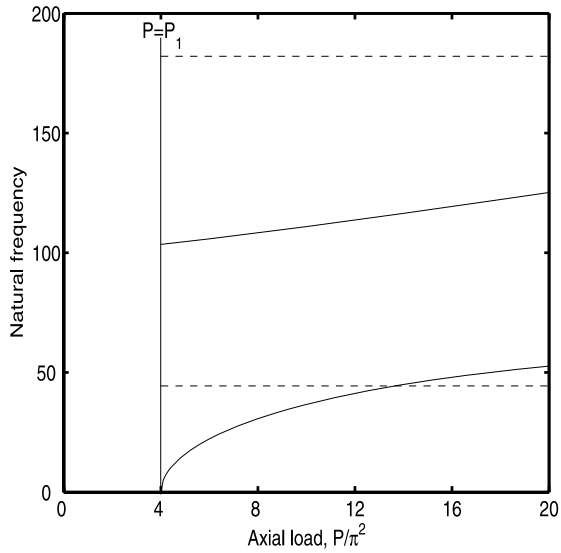

(a) Vibration around the first buckled mode

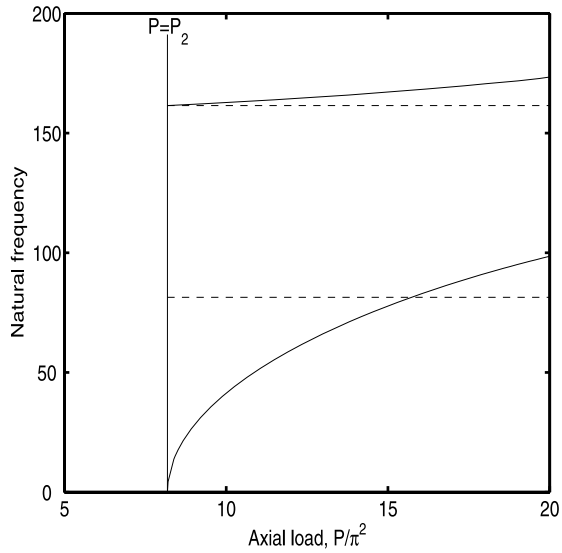

(b) Vibration around the second buckled mode

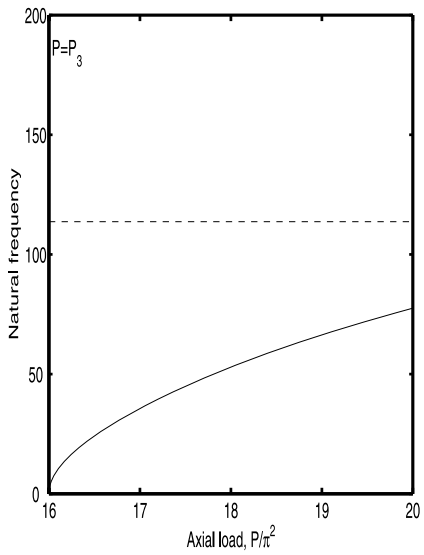

(c) Vibration around the third buckled mode

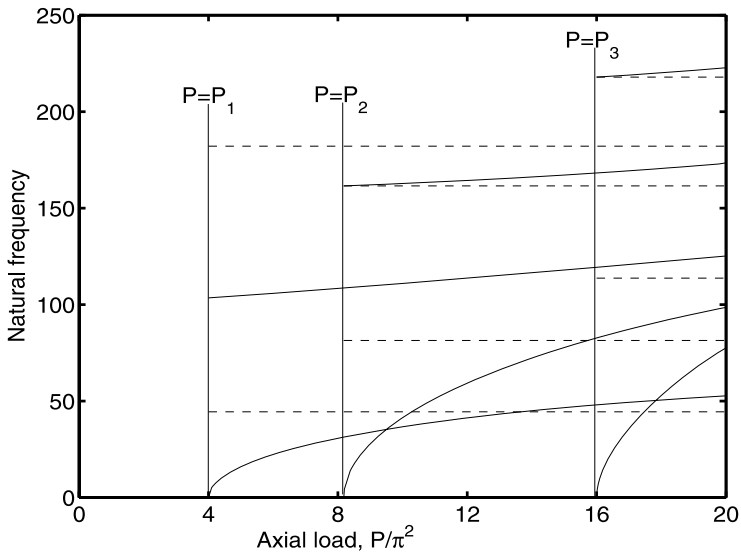

(d) Vibration around all of the buckled configurations

Fig. 3 Variation of the natural frequencies of vibration around the lowest three buckled configurations of a fixed–fixed beam

$$d_1 s_1^2 \sin s_1 + d_2 s_1^2 \cos s_1 - d_3 s_2^2 \sinh s_2 - d_4 s_2^2 \cosh s_2 = 0. \quad (65)$$

Equations (62)–(65) along with either (50) or (51) represent an eigenvalue problem for the vibration of hinged–hinged buckled beams. For this particular

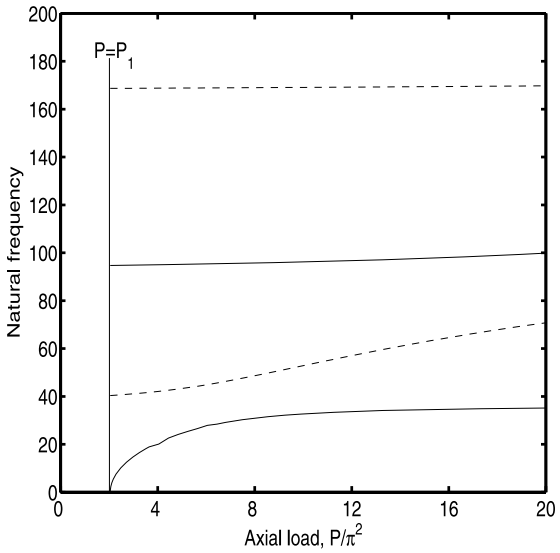

(a) Vibration around the first buckled mode

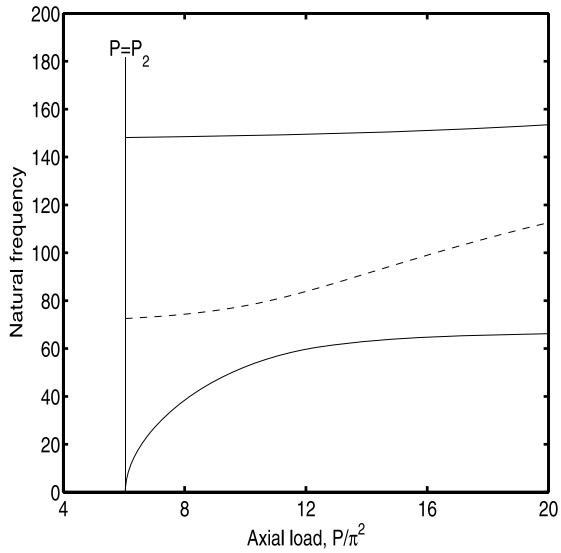

(b) Vibration around the second buckled mode

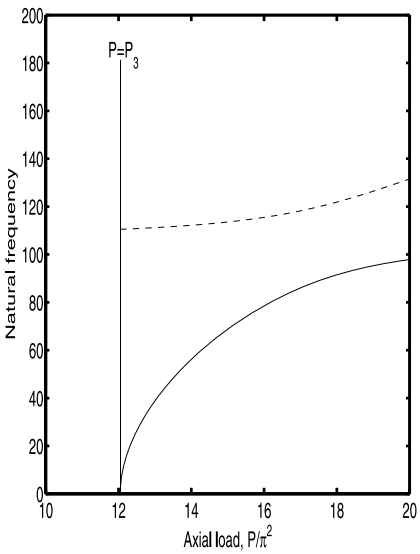

(c) Vibration around the third buckled mode

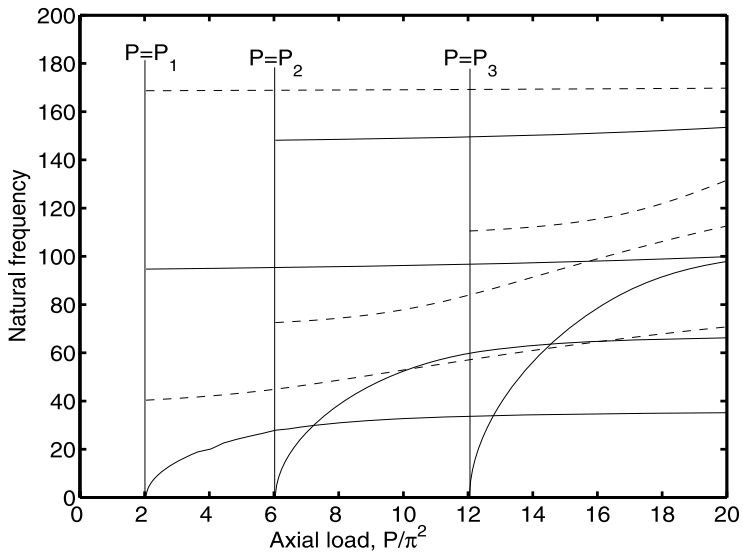

(d) Vibration around all of the buckled configurations

Fig. 4 Variation of the natural frequencies of vibration around the lowest three buckled configurations of a fixed–hinged beam

case, the eigenvalue problem yields simple formulas for the natural frequencies and mode shapes of even and odd modes as presented next.

For odd modes, where (50) holds, the characteristic equation governing the natural frequency of the only odd mode is given by

$$\omega^2 = \frac{1}{2}c^2\lambda^4 \quad \text{or} \quad \omega^2 = 2\lambda^4\left(\frac{P}{\lambda^2} - 1\right). \tag{66}$$

We note that ω^2 is always positive because P is greater than λ^2 in the postbuckling domain. Solving for the corresponding mode shape, we obtain

$$\phi(x) = \psi'' \quad \text{or} \quad \phi(x) = \sin m\pi x, \quad m = 1, 2, 3, \ldots. \tag{67}$$

For even modes, where (51) holds, the equation governing the natural frequencies can be obtained by demanding that the determinant of the coefficient matrix of (62)–(65) equals to zero. The result is

$$\left(\omega^2 + 4\lambda^4\right)\sin s_1 \sinh s_2 = 0. \tag{68}$$

There are three possibilities: the first yields a negative root that is given by

$$\omega^2 + 4\lambda^4 = 0 \quad \text{or} \quad \omega^2 = -\frac{1}{4}\lambda^4. \tag{69}$$

The second yields

$$\sin s_1 = 0 \quad \text{or} \quad s_1 = n\pi. \tag{70}$$

And the third yields

$$\sinh s_2 = 0 \quad \text{or} \quad s_2 = in\pi. \tag{71}$$

Substituting (70) and (71) into (46), using the fact that $\lambda = m\pi$, and solving for ω, we obtain

$$\omega^2 = n^2\pi^4\left(n^2 - m^2\right) \tag{72}$$

where n and m are two integers denoting the vibration mode and the buckling mode, respectively. When $n > m$, ω^2 is positive and (70) holds. When $n < m$, ω^2 is negative and (71) holds.

Solving the eigenvalue problem for the constants d_i yields

$$d_2 = d_4 = 0 \quad \text{and} \quad d_1 = -\frac{\sinh s_2}{\sin s_1}d_3. \tag{73}$$

As a result, the mode shapes can be expressed as follows:

$$\phi(x) = d_3\left(\frac{-\sinh s_2}{\sin s_1}\sin s_1 x + \sinh s_2 x\right). \tag{74}$$

To investigate the stability of buckled configurations of hinged–hinged beams, we solve for the mode shapes corresponding to negative eigenvalues and determine whether they are physical or not. For the first case, where ω is given by (69), we obtain

$$s_1 = \frac{1}{2}\lambda \quad \text{and} \quad s_2 = \frac{1}{2}i\lambda \tag{75}$$

where $i = \sqrt{-1}$. Substituting (75) into (74), we obtain

$$\phi(x) = 0$$

which implies that this negative root corresponds to a vanishing mode shape. For the third case, we substitute (71) into (74) and obtain

$$\phi(x) = \sin n\pi x$$

which is physical, and hence the second and higher-order buckling modes are unstable.

Figure 5 presents variation of the natural frequencies of vibration around the first, second, and third buckled shapes with the applied axial load for hinged–hinged beams. Many internal resonances might be activated among vibration modes around the same buckled configuration and different buckled configurations. A one-to-one internal resonance among the three modes ϕ_{31}, ϕ_{12}, and ϕ_{13} might be activated at $P \approx 13\pi^2$, as shown in Fig. 5(d).

5 Preliminary dynamic results

We present preliminary results for the nonlinear interaction between the vibration modes around the first and second buckled configurations. As can be seen from Fig. 3, there is a possibility of activating a one-to-one internal resonance between the lowest vibration modes around the first and second buckled configurations at $P = 9.5\pi^2$. We consider the case in which the beam is excited with a uniform lateral harmonic force having a frequency close to ω_{11}; that is, the lowest natural frequency around the first buckled configuration. We found three different responses: (1) a local attractor around the first buckled configuration, (2) a chaotic snap-through motion among all buckled configurations, including the second one, and (3) a snap-through motion between the two second buckled configurations. Snap shots of these motions are shown in Fig. 6. We emphasize that antisymmetric modes cannot be excited directly by the external uniform load

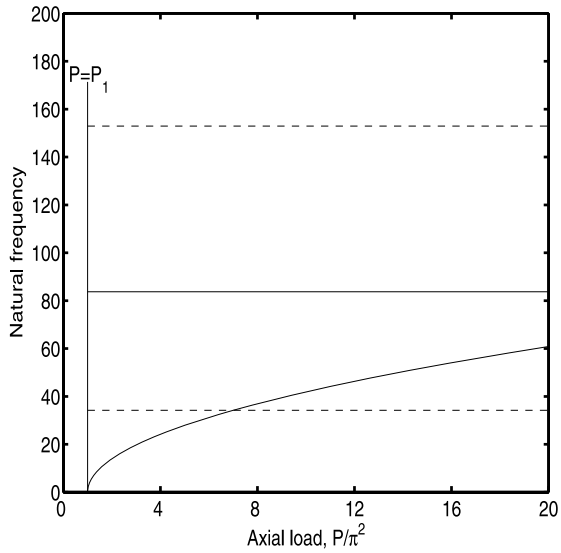

(a) Vibration around the first buckled mode

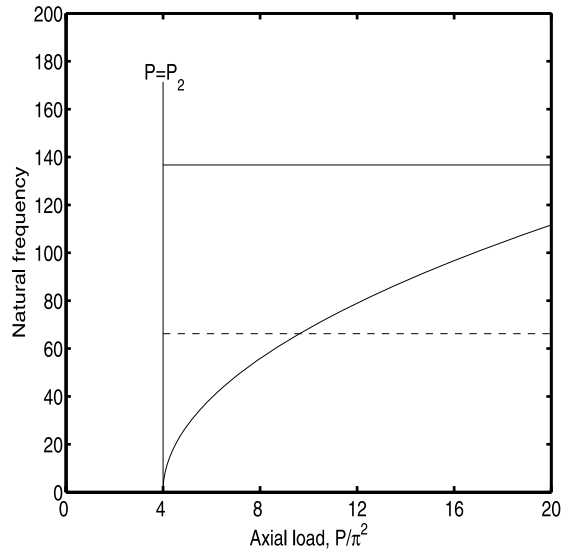

(b) Vibration around the second buckled mode

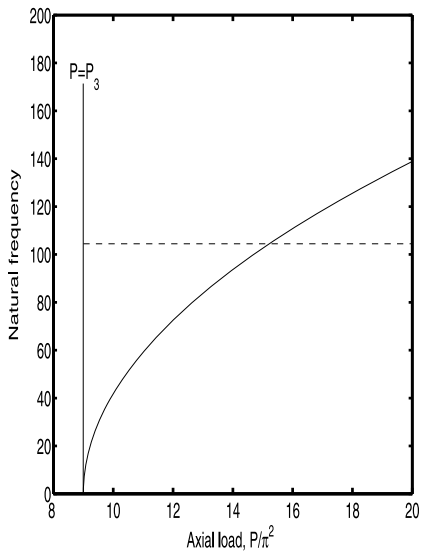

(c) Vibration around the third buckled mode

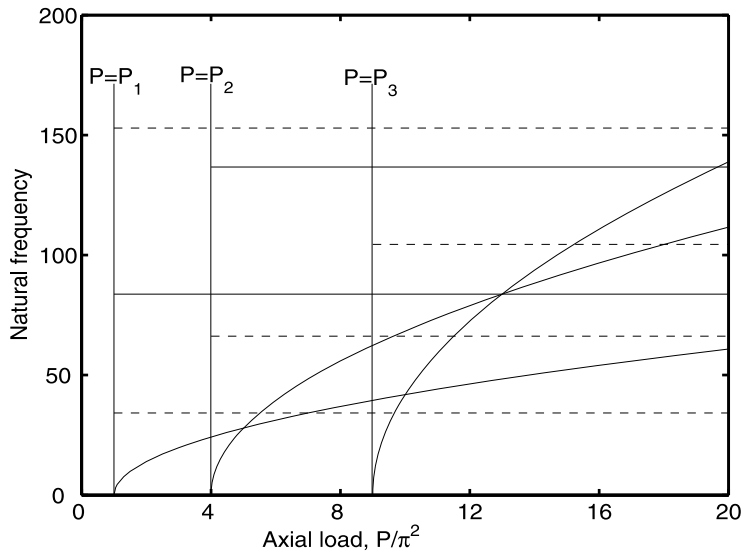

(d) Vibration around all of the buckled configurations

Fig. 5 Variation of the natural frequencies of vibration around the lowest three buckled configurations for a hinged–hinged beam

because its projections onto these modes are zero. The only way to excite these modes is via internal resonance. Therefore, these preliminary results demonstrate the possibility of the interaction between vibration modes around different buckled configurations. These results open the door for more theoretical and

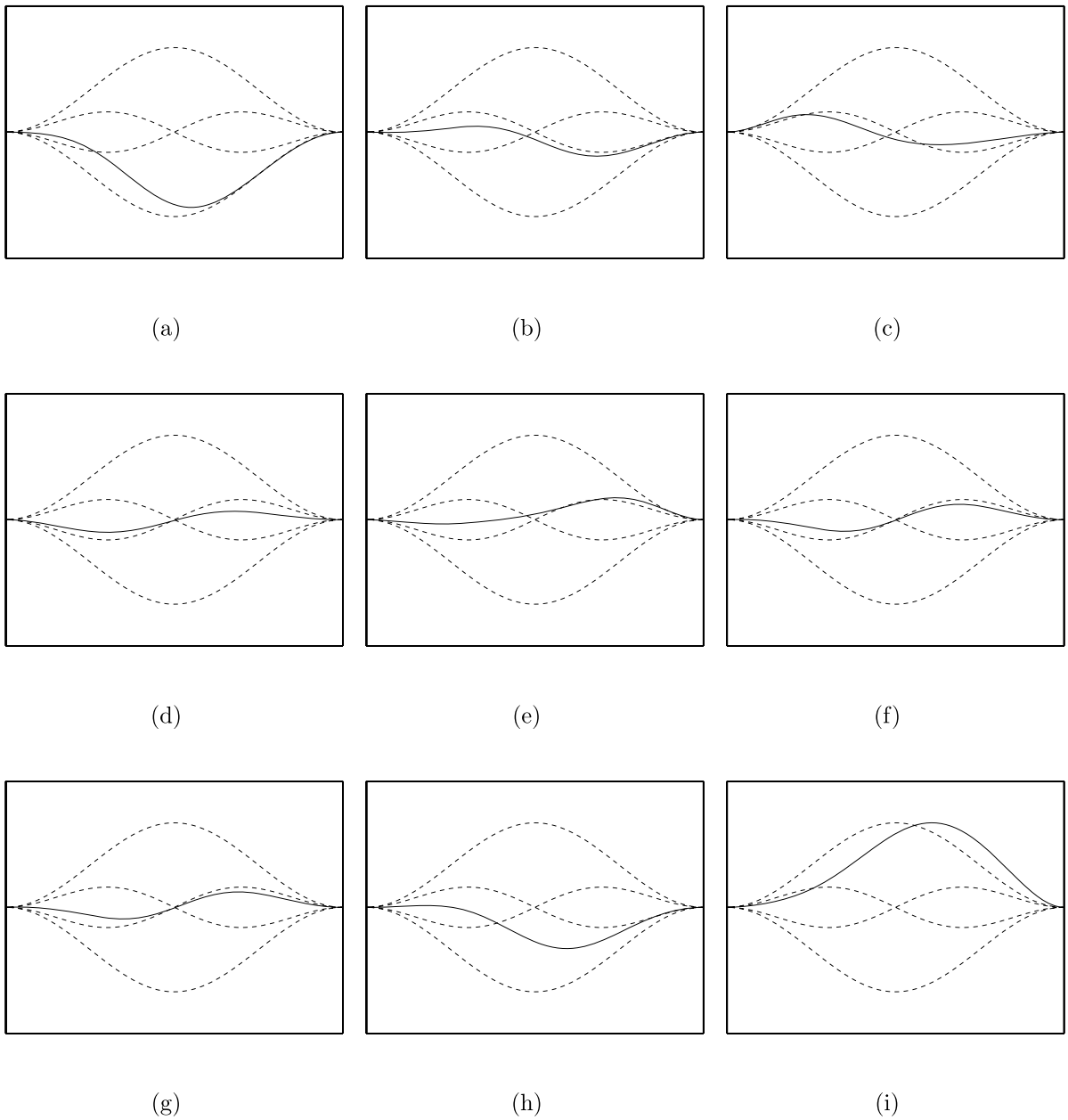

Fig. 6 Snap shots of the dynamic displacement $w(x,t)$ showing the interaction between vibration modes around different buckled configurations

experimental exploration of the complex and rich dynamics of buckled beams.

6 Conclusions

We presented an exact solution for the postbuckling of fixed–fixed, fixed–hinged, and hinged–hinged beams taking into account the geometric nonlinearity arising from midplane stretching. A closed-form expression is obtained for the postbuckling configuration as a function of the applied axial load. The critical buckling loads and their associated mode shapes are obtained as a byproduct.

We investigated the dynamic stability of the buckling modes of beams with various boundary conditions. We found out that the first buckling mode is a stable equilibrium position for all boundary conditions. Buckled configurations beyond the first bucking mode of fixed–fixed, fixed–hinged, and hinged–hinged beams are found to be unstable equilibrium positions. As a result, when the applied axial load goes beyond the second buckling load, the beam exhibits stable and unstable equilibrium positions, and hence it has a rich and complex dynamics. We calculated the lowest natural frequencies of vibration around each of the first three buckled configurations. We found out that many internal resonances might be activated among vibration modes not only around the same buckled configuration, but also around different buckled configurations. We presented preliminary results for the dynamic response in the case of a one-to-one internal resonance between the first vibration modes around the first and second buckled configurations of a fixed–fixed beam. The results demonstrate that energy is being continuously exchanged between these coupled modes. These results open the door for further investigations into the rich and complex dynamics of buckled beams.

Acknowledgements The authors express their deep thanks to the valuable comments made by the reviewer.

Appendix A: Orthogonality condition for the buckling problem

We derive the orthogonality condition for the buckling problem. We let ψ_1 and ψ_2 be the two buckled mode shapes corresponding to the two buckling eigenvalues λ_1 and λ_2, respectively. Then it follows from (12) that

$$\psi_1^{iv} + \lambda_1^2 \psi_1'' = 0, \tag{76}$$

$$\psi_2^{iv} + \lambda_2^2 \psi_2'' = 0. \tag{77}$$

Multiplying (76) with ψ_2 and (77) with ψ_1, subtracting the results, and integrating the outcome over the domain, we obtain

$$\int_0^1 \left(\psi_2 \psi_1^{iv} + \lambda_1^2 \psi_2 \psi_1'' - \psi_1 \psi_2^{iv} - \lambda_2^2 \psi_1 \psi_2''\right) dx = 0. \tag{78}$$

Integrating (78) by parts, we have

$$\left[\psi_2 \psi_1''' - \psi_2' \psi_1'' - \psi_1 \psi_2''' + \psi_1' \psi_2'' + \lambda_1^2 \psi_2 \psi_1' - \lambda_2^2 \psi_1 \psi_2'\right]_0^1 + \left(\lambda_2^2 - \lambda_1^2\right) \int_0^1 \psi_1' \psi_2' \, dx = 0. \tag{79}$$

The term in brackets vanishes for boundary conditions of the fixed–fixed, fixed–hinged, and hinged–hinged beams. Hence,

$$\left(\lambda_2^2 - \lambda_1^2\right) \int_0^1 \psi_1' \psi_2' \, dx = 0. \tag{80}$$

When $\lambda_2 \neq \lambda_1$, (80) yields the orthogonality condition

$$\int_0^1 \psi_1' \psi_2' \, dx = 0. \tag{81}$$

References

1. Emam, S.A.: A theoretical and experimental study of nonlinear dynamics of buckled beams. PhD dissertation, Virginia Polytechnic Institute and State University, Blacksburg, VA (2002)
2. Nayfeh, A.H., Pai, P.F.: Linear and Nonlinear Structural Mechanics. Wiley-Interscience, New York (2004)
3. Fang, W., Wickert, J.A.: Postbuckling of micromachined beams. J. Micromach. Microeng. **4**, 116–122 (1994)
4. Li, S., Zhou, Y.: Free vibration of heated Euler–Bernoulli beams with thermal postbuckling deformations. J. Therm. Stresses **27**, 843–856 (2004)
5. Nayfeh, A.H., Kreider, W., Anderson, T.J.: Investigation of natural frequencies and mode shapes of buckled beams. AIAA J. **33**, 1121–1126 (1995)